CHAPTER TWO

Terrestrial water storage

Manuela Girotto[1,2,3] and Matthew Rodell[4]
[1]Global Modeling and Assimilation Office, NASA Goddard Space Flight Center, Greenbelt, MD, United States
[2]GESTAR, Universities Space Research Association, Columbia, MD, United States
[3]Department of Environmental Science, Policy, and Management, University of California, Berkeley, CA 94720, United States
[4]Hydrological Science Lab, NASA Goddard Space Flight Center, Greenbelt, MD, United States

2.1 Terrestrial water storage components

Terrestrial water storage (TWS) is a dynamic component of the hydrological cycle that exerts important controls over the water, energy, and biogeochemical fluxes, thereby playing a major role in Earth's climate system (Syed et al., 2008; Famiglietti, 2004). TWS is defined as the summation of all water stored above and below the land surface. This includes surface waters, soil moisture, groundwater, snow, ice, and water stored in vegetation. The variability of TWS tends to be dominated by surface waters in wet, tropical regions such as the Amazon, by soil moisture and groundwater in mid-latitudes, and by snow and ice in polar and alpine regions (Rodell and Famiglietti, 2001). The variations in water stored in vegetation are small compared to those of the other TWS components, therefore they are typically assumed to be negligible in TWS budget analyses (Rodell et al., 2005).

Surface waters include rivers, inland water bodies, wetlands, and inundated floodplains. Surface waters supply agricultural and energy production for most regions in the tropics, and because they exist at the land–atmosphere interface they affect hydrometeorological and biogeochemical processes. Getirana et al. (2017) found that changes in surface water storage are a substantial component of TWS variability in the wet tropics (e.g., the Amazon), where major rivers flow over arid regions (e.g., the Nile River in Egypt) and in subpolar regions. Conversely, changes in surface water storage are negligible in the Western United States, Northern Africa, Middle East, and Central Asia.

Soil moisture is defined as the water stored in the unsaturated zone of the soil. It controls the partitioning of rainfall into runoff and infiltration,

Extreme Hydroclimatic Events and Multivariate Hazards in a Changing Environment.
DOI: https://doi.org/10.1016/B978-0-12-814899-0.00002-X

constrains evapotranspiration, and influences the occurrence of flood water extremes, because when the soil is saturated it cannot be infiltrated by any more water (Milly and Dunne, 1994; Crow et al., 2005; Zehe et al., 2005). Soil moisture governs the partitioning of the turbulent fluxes (latent and sensible heat); hence it affects global and regional hydrometeorological processes (Entekhabi et al., 1996; Seneviratne et al., 2010). In parts of the tropics and in the mid-latitudes, soil moisture variations are generally the largest component of seasonal terrestrial water storage changes.

Groundwater is the other major component of TWS in the mid-latitudes, where it provides domestic water to a billion people and plays a central role in agriculture and energy production (Gleeson et al., 2012; Famiglietti, 2014). This resource has received increasing attention in recent years because of the accelerated rate of depletion of major global aquifers (e.g., Rodell et al., 2009; Wada et al., 2010; Famiglietti et al., 2011; Richey et al., 2015; Girotto et al., 2017). Groundwater storage changes are rarely the dominant component of TWS variations on a seasonal basis, but they are often the dominant component on interannual to decadal timescales (Rodell and Famiglietti, 2001; Li et al., 2015).

Finally, the water stored in the form of snow or ice is the primary component of TWS in high latitude regions and mountainous regions of the mid-latitudes (Rodell and Famiglietti, 2001; Seneviratne, 2003; Getirana et al., 2017). This is because snow water storage induces significant variations in TWS due to the mass that accumulates during winter and the mass that melts during springtime. These fluctuations also affect the surface energy balance because of the changes in surface albedo (Hall et al., 1988). Accurate global estimates of snow across space and time are currently lacking due to the complexity of the terrain or inaccessibility of the regions where snow/ice is stored. For this reason, large-scale efforts for estimating snow properties must rely heavily on remote sensing (Schmugge et al., 2002; Girotto et al., 2014). Existing efforts to estimate snow water equivalent (SWE) from remote sensing include using microwave, visible and near infrared, radar, and gravimetric measurements. A dedicated snow-measuring satellite mission has not yet been launched, but efforts have begun (e.g., NASA SnowEx, https://snow.nasa.gov/campaigns/snowex) in which international teams of experts are working to devise satellite instruments capable of measuring SWE and/or snow depth from space.

2.2 Overview of the GRACE mission

The Gravity Recovery and Climate Experiment (GRACE) maps the gravity potential of the Earth. From these gravity maps scientists can infer global and regional changes of the terrestrial water storage, ice loss, and sea level change caused by the addition of water to the ocean providing a unique view of Earth's climate and have far-reaching benefits to society and the world's population. GRACE is jointly operated by NASA and the German Aerospace Center. It was launched on March 17, 2002, and it continued to perform past its nominal mission lifetime of 5 years until battery failure caused the end of the science mission in 2017. It consisted of two satellites in a tandem orbit about 200 km apart at 450–500 km altitude. Fig. 2.1 shows in a simplistic way the principle behind the gravity measurements. The two GRACE satellites flew in a tandem orbit over the Earth. In the case shown in Fig. 2.1, a mountain represents a positive mass anomaly. As the lead satellite approached the mountain it was pulled toward it because of the gravitational force exerted by the mass anomaly. Thus, the distance between the two satellites increased. As the trailing satellite approached the mountain, it was pulled toward the anomalous mass while the lead satellite was held back by the same mass anomaly, and the distance between the satellites decreased. Finally, as the trailing satellite moved away from the mountain, it was held back, and their distance increased again. In a nutshell, measurement of the distance (range) and changes in distance (range-rate) between the two satellites are related to the gravitational potential of earth masses. A K-band microwave tracking system continuously measures changes in the distance between the satellites with a precision better than 1 μm (Tapley et al., 2004). The measurements are so precise that mass changes associated with ocean circulation, atmospheric circulation, and terrestrial water storage redistribution can be detected by GRACE. Nongravitational accelerations are monitored by onboard accelerometers, and the precise positions of the satellites are measured via global positioning system (GPS). The monthly analysis of the range and range-rate measurements between the two satellites provides the temporal variations (i.e., anomalies) of the gravity field.

The successor of GRACE is the GRACE follow-on (GRACE-FO) mission. GRACE-FO, launched on May 22, 2018, carries on the work of its predecessor while testing a new laser ranging system designed to improve the precision of the intersatellite distance measurement.

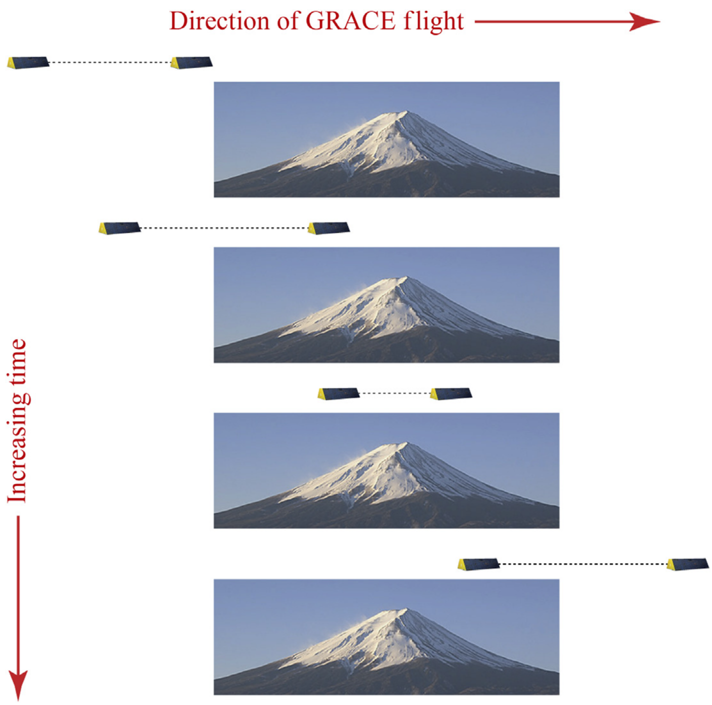

Figure 2.1 Simplified example of how the GRACE mission observed the time variable gravity field. The two GRACE satellites flew in tandem over the Earth (first panel). In this graphic the mountain represents a positive mass anomaly. As the lead satellite approached the mountain it was pulled toward it because of the gravitational force exerted by the mass anomaly. Thus, the distance between the two satellites increased (second panel). As the trailing satellite approached the mountain, it was pulled toward the anomalous mass while the lead satellite was held back by the same mass anomaly, and the distance between the satellites decreased (third panel). Finally, as the trailing satellite moved away from the mountain, it was held back, and their distance increased again (fourth panel).

2.3 Terrestrial water storage solutions

A monthly analysis of the range and range-rate measurements results in a map of temporal variations (i.e., anomalies) of the gravity fields caused by redistribution of earth masses. Masses can be static or time variable. Static masses include the total mass of the earth and mass heterogeneities that only vary on geologic timescales. This includes location of the continents, mountains, and depression in the crust. The static masses are "removed" when the long-term mean gravity field is saturated from a month solution to produce an anomaly map. The main drivers of temporal variations in the gravity field are oceanic and atmospheric circulations and redistribution of terrestrial water via the hydrological cycle. Atmosphere mass changes are removed during preprocessing using model based atmospheric pressure fields. An ocean model is used to remove high frequency (6-hourly to submonthly) wind and pressure-driven ocean motions that might otherwise alias into the monthly gravity solutions. What remains are anomalies in terrestrial water storage (TWS). Glacial isostatic adjustment must also be considered in certain regions such as Hudson's Bay in Canada, and a major earthquake can produce a significant gravitational anomaly, but the timescales of most solid earth processes are too long to be an issue.

Currently, the range-rate observations are processed using either spherical harmonics (Wahr et al., 1998) or the mass concentration (mascon, Rowlands et al., 2005) approach to produce the monthly gravity solutions.

The spherical harmonics solutions represent the gravity field via a set of coefficients (degree and order ≤ 120) of a given spherical harmonic expansion that describes the shape of the geoid (the surface of constant gravitational potential best matching the mean sea surface). The expansion coefficients can be manipulated using numerical devices such as Gaussian averaging functions in order to isolate mass anomalies (deviations from the baseline temporal mean) over regions of interest (e.g., Wahr et al., 1998). The spherical harmonic solutions have typically suffered from poor observability of east—west gradients, resulting in the so-called "stripes" that are conventionally removed via empirical smoothing and/or "destriping" algorithms (Swenson and Wahr, 2006). Although quite effective, especially for larger spatial scales, the destriping also removes some real geophysical signal along with the stripes, and the size, shape, and orientation of the signals strongly affects the effectiveness of destriping (Watkins et al., 2015). For this reason, errors in such estimates are inversely related to the size of the region, being as small as 1—2 cm equivalent height of water over continental-scale river basins, and being large enough to overwhelm the hydrology signal as the area drops below $\sim$150,000 km^2 (Rodell and Famiglietti, 1999; Wahr et al., 2006). Three centers are currently generating spherical harmonic fields: the Center for Space Research at the University of Texas; the GeoForschungsZentrum. Potsdam, Germany; and the Jet Propulsion Laboratory, California.

As an alternative to the spherical harmonic technique, the intersatellite ranging data can also be used directly to estimate regional "mass concentrations" (mascons) without the need to first derive a global gravity field (Rowlands et al., 2005). The primary advantage of using mascons as a basis function is that each mascon has a specific known geophysical location (unlike spherical harmonic coefficients which individually have no particular localization information). Mascons take advantage of this convenient property to specify a priori information (constraints) during the data inversion to internally remove the correlated error in the gravity solution. So, unlike the spherical harmonic solutions, the constrained mascon solutions typically do not need to be destriped or smoothed. The mascon approach also allows a better separation of land and ocean signals. Mascons solutions are currently freely available from different centers such as the Jet Propulsion Laboratory, California (Watkins et al., 2015); the Goddard Space and Flight Center, Maryland (Luthcke et al., 2013); and the Center for Space Research, Texas (Save et al., 2012).

2.4 Extremes in water storage

Extremes in water storage often are manifested as droughts and flooding events, driven by the surplus or deficit of water stored in a river basin or an aquifer. Understanding the spatial and temporal extent of these hydrologic extremes is critical for water resources management, hazard preparedness, and food security (Diffenbaugh and Scherer, 2011; D'Odorico et al., 2010). Few hydrologic observing networks yield sufficient data for comprehensive monitoring of changes in the total amount of water stored in a region (Rodell and Famiglietti, 2001). GRACE observations have helped to fill this gap. They have been used to characterize regional flood potential (e.g., Reager and Famiglietti, 2009) and to assess wetness and drought for the US Drought Monitor (e.g., Houborg et al., 2012). Furthermore, as an integrated measure of all surface and groundwater storage changes, GRACE data implicitly contains a record of seasonal to interannual water storage variations that can likely be exploited to lengthen early warning periods for regional flood and drought prediction (Thomas et al., 2014; Sun et al., 2017a,b). The next two subsections will provide a review of the extreme water storage events identified by the GRACE mission along with the potential for predictability.

2.4.1 Droughts

A meteorological drought is defined as an extended period of low precipitation, whereas hydrological droughts are generally defined as extended periods of water storage deficits leading to low streamflow. Satellite gravimetry is the only remote sensing technique able to monitor the water storage in a holistic manner. For this reason, GRACE data have been investigated alone, or in combination with land surface models, to analyze worldwide hydrological drought conditions and provide new methods to monitor droughts (Zhao et al., 2017). Moreover, GRACE can contribute to regional drought characterization by measuring water storage deficits in previously identified, drought-stricken areas. The duration and magnitude of the deficits can serve as metrics to help quantify hydrological drought severity (Thomas et al., 2014). This subsection provides a review of previous studies that used GRACE to quantify, analyze, and monitor droughts.

Recent studies have investigated the potential for using GRACE information to monitor droughts. In addition to Thomas et al. (2014) and Houborg et al. (2012), Cao et al. (2015) introduced the total storage deficit index, derived from the GRACE-recovered terrestrial water storage changes, to analyze drought characteristics in arid northwestern China. Yirdaw et al. (2008) employed the total storage deficit index, to characterize the 2002/2003 drought episode and generate a pictorial representation of the long-term dryness and wetness within the Saskatchewan River Basin in Canada. Yi and Wen (2016) established a GRACE-based hydrological drought index for drought monitoring in the continental United States from 2003 to 2012. Kusche et al. (2016) mapped the probabilities of extreme continental water storage changes form space gravimetry. They derived hot spot regions of high probability of peak anomalous water storage. Using the GRACE-derived TWS anomaly index, Wang et al. (2014) compared the precipitation anomaly index and the vegetation anomaly index to analyze drought events in the Haihe River Basin, China, from January 2003 to January 2013. Thomas et al. (2014) described a quantitative approach (based on water storage deficits) to measure the occurrence, severity, frequency, magnitude, and duration of hydrological droughts based on the GRACE-derived TWS (Sun et al., 2018).

Combined satellite/model drought monitoring tools are also becoming more common. Data assimilation systems merge observations with physically based models, using the model to provide spatially and temporally complete estimates of all drought-relevant hydrologic variables and the observation record to correct for model errors (Anderson et al., 2012). In particular, the application of the GRACE data assimilation approach for drought monitoring has recently been explored by NASA-funded investigations (Houborg et al., 2012; Rodell, 2012). These result in surface and root-zone soil moisture and groundwater drought indicators based on GRACE data assimilation results, and to evaluation of those indicators as inputs to the USDM products. Houborg et al. (2012) and Li et al. (2012) used GRACE data assimilation to evaluate its potential for developing new drought indicator products to serve as baselines for the Drought Monitor maps. The assimilation downscaled (in space and time) and disaggregated GRACE data into finer scale TWS components, which exhibited significant changes in their dryness rankings relative to those without data assimilation, suggesting that GRACE data assimilation could have a substantial impact on drought monitoring (Li et al., 2012; Houborg et al., 2012). The weekly indicators are available on the National Drought Mitigation Center's website (http://drought.unl.edu).

2.4.1.1 Major world droughts

Thomas et al. (2014) presented gravity-based measurements of water storage anomalies during recent droughts. They used GRACE to explore how hydrological droughts may be better characterized while estimating the associated regional water storage deficit. The average storage deficit during drought events can be identified using (1) the storage deficit as a negative departure from the seasonal cycle and (2) the drought duration as the number of months with continuous deficits (Thomas et al., 2014). In essence, the average storage deficit is an arithmetic mean of the storage deficit observed during a given drought event and it is used as a measure of drought intensity. Based on these definitions of storage deficit and drought duration, Humphrey et al. (2016) provided a review of all drought events identified in the GRACE period from 2002 to 2015. Fig. 2.2 shows the maximum average storage deficit ever observed for all drought events identified in April 2002–January 2017 by the GRACE record as derived by Humphrey et al. (2016). The year corresponding to this maximum is depicted in Fig. 2.2B. Here, we group these major drought events by continents. We discuss the potential for using GRACE data and models (via data assimilation) to improve predictability of these droughts events in the next section.

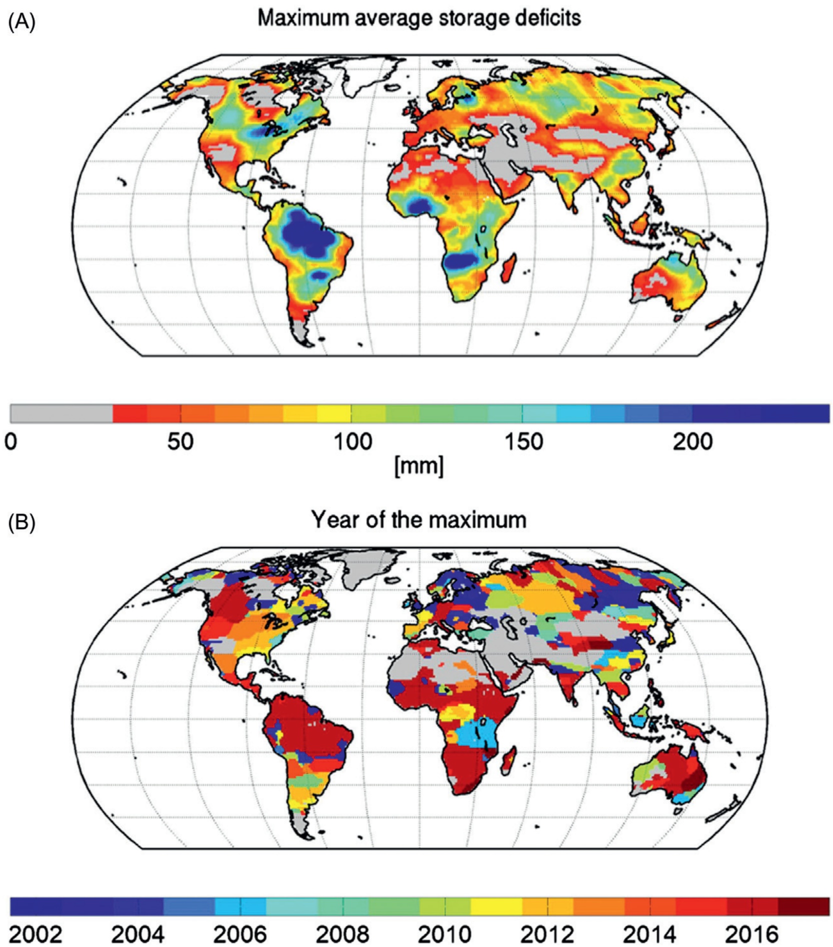

Figure 2.2 (A) Maximum value of the average storage deficit observed in the period April 2002–August 2015, expressed in mm of equivalent water height. (B) Year corresponding to the maximum value of the average storage deficit, showing only regions with a deficit larger than 30 mm. *Adapted from Humphrey, V., Gudmundsson, L., Seneviratne, S.I., 2016. Assessing global water storage variability from GRACE: Trends, seasonal cycle, subseasonal anomalies and extremes. Surveys Geophys., 37(2), 357–395.*

South America

The Amazon River water storage during year 2016 was one of the lowest during the GRACE record (Fig. 2.2). Other droughts, not shown, are identified for this region, such as the 2004–08, and 2010 dry-period reported in the works of Humphrey et al. (2016), Frappart et al. (2012), and Thomas et al. (2014). Getirana (2016) uses GRACE to identify a water loss rate of 26.1 cm/year for southeastern Brazil over the period from 2012 to 2015. Drought events in the Amazon River basin were shown to be related to precipitation deficits and to the El Niño Southern Oscillation (ENSO, Davidson et al., 2012; Frappart et al., 2012). The Amazon basin extreme droughts cause ineffective hydropower production. In fact, water storage droughts in this region cause massive agricultural losses, water supply restrictions, and energy rationing.

The 2008–12 La Plata basin (Argentina) drought is also seen in Fig. 2.2. Chen et al. (2010) identify the onset of this drought using GRACE. In their work, GRACE revealed details of the temporal and spatial evolution of this drought, with onset around austral spring 2008 in the lower La Plata basin, which spread to the entire La Plata basin. Wetness and drought in this region is correlated with ENSO, with dry and wet seasons corresponding to ENSO events, respectively (Chen et al., 2010; Abelen et al., 2015; Sordo-Ward et al., 2017).

North America

The 2012–15 drought in the Central Valley of California is also shown in Fig. 2.2. This drought reduced natural recharge to the aquifers and caused low annual snow accumulations in the Sierra Nevada Mountains (Margulis et al., 2016). Groundwater acts as the key strategic reserve in times of drought and the Central Valley is the most productive agricultural region for fresh produce in the United States (Faunt et al., 2009). Excessive groundwater pumping during a period of meteorological drought can cause unrecoverable losses at aquifer storage capacity (Faunt et al., 2009; Famiglietti et al., 2011; Famiglietti, 2014; Scanlon et al., 2012a,b). For example, Famiglietti et al. (2011) estimate a depletion in groundwater that totaled 20 km^3 of water during 2012–15. Continued groundwater depletion at this rate may well be unsustainable, with potentially dire consequences for the economic and food security of the United States (Famiglietti et al., 2011). Groundwater depletion can cause significant land subsidence (Galloway and Riley, 1999). The analysis of TWS for the entire GRACE record also indicates dry episodes for previous years over the southwestern United States. For example, Scanlon et al. (2012a) and Famiglietti et al. (2011) report that groundwater depletion was observed in the Central Valley during the drought period from April 2006 through September 2009.

Notably, most of the US experienced droughts in 2012 (Fig. 2.2). The US Drought Monitor (Schmugge et al., 2002) estimated that over three-quarters of the contiguous US experienced at least abnormally dry conditions by the summer's end with nearly half of the region, especially the Great Plains, experiencing severe drought (Hoerling et al., 2014). This period lacked the usual abundance of slow-soaking precipitation-bearing systems and evening thunderstorms along the Great Plains, and as a result, surface moisture conditions greatly deteriorated. GRACE data was used to identify this massive event (Humphrey et al., 2016). Most importantly, GRACE TWS data helped identify the recovery time. In March 2013, heavy winter rains broke a 3-year pattern of meteorological drought in much of the southeastern United States, while drought conditions still plagued the Great Plains and other parts of the United States. Chew and Small (2014) found that standard drought indices misrepresent the recovery time from the drought, putting it much earlier than the one obtained with the auxiliary information of GRACE TWS. Accurate understanding of drought onset and recovery time is critical because drought impacts grain and wheat prices (Boyer et al., 2013). A large disruption to production of these crops can have a substantial impact on international grain markets. Also visible in Fig. 2.2 are the droughts during the years 2007–09 over the eastern United States. Houborg et al. (2012) demonstrated the capabilities of using GRACE data assimilation for characterizing the hydrological drought (more discussion in Section 2.4.1.2). Furthermore, the 2010–13 drought in Texas is shown in Fig. 2.2 and was described by Long et al. (2014).

Africa

Fig. 2.2 identifies the 2006–07 dry conditions over an extended area around the Lake Victoria (Swenson and Wahr, 2009). The 2006–08 Zambezi basin (Thomas et al., 2014) and Lake Victoria droughts are captured as one large-scale and spatially contiguous event. Droughts in East Africa are recurring phenomena with significant humanitarian impacts. GRACE total water storage estimates reveal that water storage declined in much of East Africa by up to 60 mm/year (Swenson and Wahr, 2009) during the 2006–07 drought. The complex and highly variant nature of many hydrometeorological drivers such as ENSO, sea surface temperature (SST), and land–atmosphere feedback adds to the daunting challenge of drought monitoring and forecasting in Africa. The 2010–11 drought of the Horn of Africa is not shown in Fig. 2.2 but it was identified using GRACE in previous studies (e.g., Anderson et al., 2012) to characterize its temporal and spatial evolution.

Eurasia

Hydrological droughts are common in Europe, and several episodes of severe droughts, including the 2003 drought (spreading across western and central Europe) and the 2007–08 droughts (affecting southern and southwestern Europe) were detected by GRACE TWS (Li et al., 2012). In particular, the 2003 event was associated with the 2003 European heat wave (Rebetez et al., 2006). For most of Europe, TWS values were relatively high at the beginning of 2003 due to heavy precipitation in the summer and autumn of 2002, but they decreased very rapidly in the period February–August, resulting in very dry conditions during the entire summer of 2003. The soil drying in 2003 exceeded the long-term average by far (García-Herrera et al., 2010). Following the 2003 drought and heat wave, forest fires burned a large area of Siberia (García-Herrera et al., 2010). Drought conditions can also be found in northern India for the period 2009–10 (Fig. 2.2). The year 2009 was the driest year of the decade for this region in terms of precipitation (Chen et al., 2014) and resulted in higher groundwater abstraction rates (Rodell et al., 2009).

Fig. 2.2 identifies the 2004 drought in southeast China, around the Yangtze River basin. The Yangtze River is experiencing an increasing trend in terms of the frequency of extreme events (Dai et al., 2008), which often leads to severe reductions in crop outputs, along with other related social and economic losses (Chao et al., 2016). Other severe drought events in 2006 and 2011 were identified (Sun et al., 2018). Previous works based on the analysis of GRACE data quantify a terrestrial water storage deficit of −621, −617, and −192 mm for the 2004, 2006, and 2011 droughts, respectively (Chao et al., 2016; Sun et al., 2018).

The Sumatra region exhibits a minimum in 2004 (Fig. 2.2). However, this is an artifact caused by the 2004 earthquake, with GRACE observing changes in the gravity field due to crustal dilatation and vertical displacement of Earth's layered density structure (Han et al., 2006).

Australia

In Australia, multiyear droughts have been related to precipitation deficits (García-García et al., 2011). Van Dijk et al. (2013) explained drivers of the drought and its impacts. These were analyzed using climate, water, economic, and remote sensing data combined with biophysical modeling. ENSO explained two-thirds of the rainfall deficit, and a contribution of global climate change remains plausible. The millennium drought (2001–09) was the worst drought on record for southeast Australia

(Van Dijk et al., 2013). It has led to the almost complete drying of surface water resources, which account for most of the water used for irrigation and domestic purposes. Using GRACE data, Leblanc et al. (2009) showed the propagation of the water deficit through the hydrological cycle and the rise of different types of drought.

2.4.1.2 The potential for using GRACE in monitoring and predicting droughts

Currently, standard drought quantitation methods and products including the US Drought Monitor (USDM) rely heavily on in situ observations of precipitation, streamflow, snowpack data, and subjective human-based judgments (Rodell, 2012). USDM drought maps are published on a weekly basis by a team of authors and widely considered to be the premier US drought products available for use by governments, farmers and other stakeholders, and the public, despite limited groundwater and soil moisture data as direct inputs. Although meteorological drought is defined as an extended period with deficient precipitation, hydrological and agricultural droughts are also influenced by precursor conditions of groundwater and soil moisture. Surface moisture conditions can fluctuate quickly with the weather, while the deeper components of TWS (e.g., groundwater) are well suited to drought quantification, particularly hydrologic droughts, because they integrate meteorological conditions over timescales of weeks to years (Rodell, 2012). Prior to USDM use of GRACE data assimilation-based drought indices (Houborg et al., 2012), drought products did not incorporate systematic observations of soil moisture, groundwater, or total TWS. Groundwater storage and shallow and deep soil moisture are still major gaps in current drought monitoring capabilities and monitoring of droughts has suffered from the lack of reliable information on the water stored below the uppermost soil layer. Remote sensing-based drought indices have opened a new path forward in drought monitoring and detection (Niemeyer, 2008), allowing accurate spatial information to be obtained with global or regional coverage with high reliability and a high repetition rate (Sun et al., 2018). In particular, since GRACE measures the water storage changes in the entire profile, it provides valuable information on drought conditions beyond what can be seen at the surface (Li et al., 2012). Furthermore, given that GRACE offers information on the total water storage deficit it can be used to estimate the amount of water (precipitation) needed to recover from drought events (Thomas et al., 2014; AghaKouchak et al., 2014).

2.4.2 Floods

Flood events are projected to become more frequent as global warming amplifies the atmosphere's water holding capacity, increasing the occurrence of extreme precipitation events (Slater and Villarini, 2016; Groisman et al., 2012; Wang et al., 2017a,b). Many countries have developed flood alert systems (Molodtsova et al., 2016), such as the European Flood Alert System (Bartholmes et al., 2009) and the US National Weather Service Automated Flood Warning System (Scawthorn, 1999). While most of these warning systems rely on a dense network of gauging stations, a significant portion of the economic losses caused by floods occur in developing countries where ground flood monitoring and management programs are still inefficient (Molodtsova et al., 2016). To augment ground-based observations, flood monitoring has increasingly relied on products based on space-borne sensor observations. Among the remote sensing products that have been used for flood monitoring, data from the GRACE mission are unique because the total amount of terrestrial water can be directly measured (Molodtsova et al., 2016). The terrestrial water storage signal relates to the ability of the land surface to absorb and process water and accounts for the water in plants, groundwater, soil moisture, and snow (Reager and Famiglietti, 2009). Over the course of a year, a region can transition between its minimum and maximum TWS due to the annual cycle of precipitation. When the region is near the maximum, it can store and process only a finite amount of water before the saturated ground will force additional precipitation to run off (Reager and Famiglietti, 2009). Generally, the land surface modulates the connection between precipitation and runoff generation through two basic mechanisms: infiltration limitation and saturation excess. During floods, one of these two mechanisms is typically identified as a driver based on the preflood conditions and the nature of the precipitation event (Reager et al., 2015). That is, the prerainfall event wetness of a watershed can determine its response to rainfall (Sayama et al., 2011; Brutsaert, 2008; Kirchner, 2009), leading to variability in flood generation (Li and Simonovic, 2002). Slater and Villarini (2016) show that flood patterns are dependent on the overall wetness and potential water storage, with fundamental implications for water resources management, agriculture, insurance, navigation, ecology, and populations living in flood-affected areas.

2.4.2.1 Flood potential from GRACE

Reager and Famiglietti (2009) introduced the concept of "flood potential" to highlight the information relevant for regional flooding contained in the GRACE extreme (wet) TWS values. TWS that is near its maximum can be a harbinger of future flood events at several months lead time (Reager and Famiglietti, 2009). The concept of flood potential has been used in several studies (Section 2.4.2.2) to analyze flood risk in different watersheds around the world.

Reager and Famiglietti (2009) assume that the regional storage capacity can be approximated by the historic record maximum in the GRACE TWS storage anomaly time series to give a quantitative estimate (in cm) of the saturation point of the regional land surface. In a nutshell, GRACE time series can be used to calculate an effective maximum storage capacity in each region. Reager and Famiglietti (2009) isolate, temporally and spatially, those months in which a high percentage of the storage capacity is achieved and high precipitation continues. Finally, they normalized this new dataset to remove regional heterogeneity and create a global flood potential index. The resulting flood potential amount is the quantity of incoming water that exceeds the storage capacity for the current month based on the regionally observed storage anomaly maxima. Similar to a traditional "bucket model," when this quantity exceeds zero, flooding is likely to occur.

Fig. 2.3A shows a global map of the flood index for the year 2007 as derived by Reager and Famiglietti (2009). This is compared to the Dartmouth Flood Observatory map of reported floods (Fig. 2.3B). The Dartmouth Flood Observatory catalogues historic floods based on satellite observations, weather service, and news reports (https://www.dartmouth.edu/~floods/). The red areas in Fig. 2.3B indicate observed floods during 2007. While the GRACE derived flood index (Fig. 2.3A) misses some flooded regions in Africa and Asia, it is generally successful at predicting large-scale flood-affected areas. The index captures the general patterns of flooding on most continents, and captures some rather high spatial resolution structure, including events on the southernmost tip of Africa and the unique "T" shape of Mississippi river flooding (Reager and Famiglietti, 2009). Furthermore, Reager et al. (2014) demonstrated the ability of the flood potential concept to derive longer lead times (as much as 5–11 months in advance) in flood warnings at a regional scale (e.g., for the Missouri, 2011, the Columbia River, 2011, and Indus River, 2010 flood events).

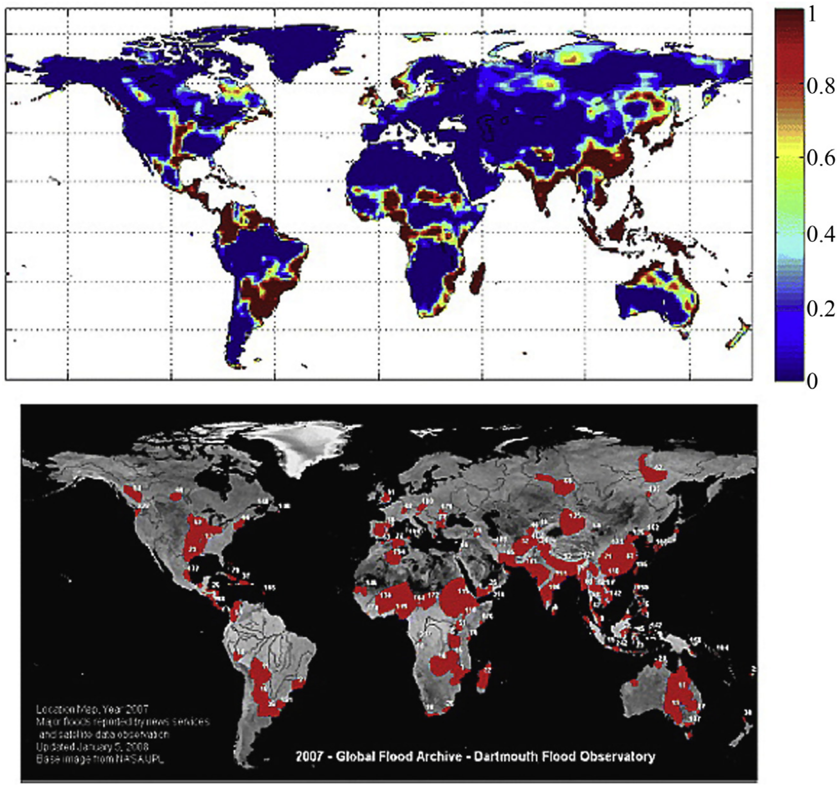

Figure 2.3 A comparison of the (top) 2007 flood index maxima and (bottom) 2007 Dartmouth Flood Observatory reported floods. *Reager, J.T., Famiglietti, J.S., 2009. Global terrestrial water storage capacity and flood potential using GRACE. Geophys. Res. Lett., 36(23):L23402.*

However, several limitations still exist for using satellite gravimetry in an operational flood prediction mode (Reager et al., 2015). The prevailing limitations are: (1) coarse spatial resolution ($\sim$150,000 km^2, Rowlands et al., 2005; Swenson and Wahr, 2006); (2) the aggregated observation of multiple water storage components (i.e., snow, soil moisture, and groundwater) as a single integrated value for each grid cell; and (3) latency in data product processing and release (2−4 months lag for GRACE and at least 10 days for GRACE-FO). These obstacles make many applications difficult, as water resource management tends to occur at small watershed scales and on daily to weekly timescales. For this reason, similarly to the drought monitoring work by Houborg et al. (2012), data assimilation can be used as a tool to partially overcome these limitations. In their work, Reager et al. (2015) assimilate GRACE data within the catchment land surface model and evaluate the assimilation scheme performance under flood conditions. The assimilation results made the model wetter in the months preceding flood, thus increasing the model capability to predict floods.

2.4.2.2 Historical flood events characterized by GRACE

The investigation of GRACE data to characterize flooding events has not been exploited as much as the characterization of drought events. This section lists historical flooding events that have been investigated with the use of GRACE data.

dutt Vishwakarma et al. (2013) discussed two major flooding events in India, one being the 2005 monsoon flooding in Mumbai and nearby states and other being the flood experienced by Bihar in 2008. GRACE detected these two flooding events at a large spatial scale. Long et al. (2014) used the flood potential index derived by Reager and Famiglietti (2009) to characterize the 2008 severe flood in southwest China. Chinnasamy (2017) developed a regression model between GRACE data and observed discharge flow. Their model was tested to predict the 2008 Koshi floods, India. Their results indicate that the saturation of water storage units in the basin play a vital role in the prediction of peak floods and their lead times. Chen et al. (2010) used GRACE to identify the Amazon River 2009 flood event, which caused many casualties, and its connection to ENSO. Sun et al. (2017a,b) used GRACE data to evaluate the flood potential index (Reager and Famiglietti, 2009) in the Yangtze River Basin of China. Zhou et al. (2017) also investigated the potentials for using GRACE data for identifying and predicting floods in the Yangtze River Basin. In particular, the 2010 flood was identified as the most serious disaster during the study period, with discharge and precipitation values 37.95% and 19.44% higher, respectively, than multiyear average values for the same period. Zhou et al. (2017) highlight that while the GRACE derived flood potential index can identify extremes for large floods, it is currently not suitable for smaller and/or short-term flood events (Sun et al., 2017a,b). Tangdamrongsub et al. (2016) used GRACE data to quantify flooding of the Tonlé ap basin, Cambodia between 2002 and 2014. For this region, the 2011 and 2013 flood events were clearly identified by GRACE. The basin-averaged TWS values for these two events were 42 cm (40% higher than the long-term mean peak value) and 36 cm (34% higher) equivalent water height, respectively. In May and June of

2011, a large flood crest moved down the Mississippi from a combination of snowmelt and heavy spring rains in the Missouri river basin. Flows in the Missouri were characterized as a 500-year event. Red River Landing, near the mouth of the Mississippi, went above flood stage on 19 March and did not fall below flood stage until 25 June. Reager et al. (2014) and Wang et al. (2014) investigated this flood event using GRACE data and they indicate that analysis of TWS observations has the potential for providing spatially distributed warning information. Similar conclusions were derived for the Columbia River flood event in May—June 2011, and the Indus River flood in 2010.

2.5 Conclusions

Extremes in water storage are often manifested as drought and flooding events, driven by the deficit or surplus of water stored in a river basin or an aquifer. These events are projected to become more frequent as a result of global warming (Pachauri et al., 2014). The existing in situ observing networks are not sufficient to detect and monitor these extremes in the total amount of water stored in a region. GRACE observations have helped to fill this information gap because GRACE has provided an unprecedented, holistic view of terrestrial water storage variations. GRACE Follow On, launched in May 2018, will extend that important data record.

GRACE has contributed to regional drought characterization by measuring water storage deficits in drought-stricken areas. It also has provided information useful for predicting regional flood potential. The concepts of flood potential and water storage deficit have been used in several studies to characterize the extremes observed by GRACE. This book chapter has reviewed many of the most significant studies.

Limitations still exist for using GRACE and GRACE Follow On data in an operational drought or flood prediction mode. The major limitations are related to the relatively coarse spatial and temporal resolutions of the GRACE observations and the fact that TWS is an aggregated observation of multiple water storage components (i.e., snow, soil moisture, and groundwater). Latency in the delivery of GRACE data is also a serious issue, but that is expected to be mitigated by the availability of low latency data products derived from GRACE Follow On (e.g., Sakumura et al., 2016). These limitations can be addressed through the combined used of observed TWS and models, that is, via data assimilation (e.g., Zaitchik et al., 2008; Girotto et al., 2016).

References

Abelen, S., Seitz, F., Abarca-del-Rio, R., Güntner, A., 2015. Droughts and floods in the La Plata basin in soil moisture data and GRACE. Remote Sensing 7 (6), 7324—7349.

AghaKouchak, A., Cheng, L., Mazdiyasni, O., Farahmand, A., 2014. Global warming and changes in risk of concurrent climate extremes: insights from the 2014 California drought. Geophys. Res. Lett. 41 (24), 8847—8852.

Anderson, R.G., Lo, M.H., Famiglietti, J.S., 2012. Assessing surface water consumption using remotely-sensed groundwater, evapotranspiration, and precipitation. Geophys. Res. Lett. 39 (16).

Bartholmes, J.C., Thielen, J., Ramos, M.H., Gentilini, S., 2009. The european flood alert system EFAS—Part 2: statistical skill assessment of probabilistic and deterministic operational forecasts. Hydrol. Earth Syst. Sci. 13 (2), 141—153.

Boyer, J.S., Byrne, P., Cassman, K.G., Cooper, M., Delmer, D., Greene, T., et al., 2013. The US drought of 2012 in perspective: a call to action. Global Food Sec. 2 (3), 139—143.

Brutsaert, W., 2008. Long-term groundwater storage trends estimated from streamflow records: climatic perspective. Wat. Resour. Res. 44, W02409.

Cao, Y., Nan, Z., Cheng, G., 2015. GRACE gravity satellite observations of terrestrial water storage changes for drought characterization in the arid land of northwestern China. Remote Sensing 7 (1), 1021—1047.

Chao, N., Wang, Z., Jiang, W., Chao, D., 2016. A quantitative approach for hydrological drought characterization in southwestern China using. Hydrogeol. J. 24 (4), 893—903.

Chen, J.L., Wilson, C.R., Tapley, B.D., Longuevergne, L., Yang, Z.L., Scanlon, B.R., 2010. Recent La Plata basin drought conditions observed by satellite gravimetry. J. Geophys. Res. Atmosph. 115 (D22).

Chen, Y., Deng, H., Li, B., Li, Z., Xu, C., 2014. Abrupt change of temperature and precipitation extremes in the arid region of Northwest China. Quatern. Int. 336, 35—43.

Chew, C.C., Small, E.E., 2014. Terrestrial water storage response to the 2012 drought estimated from GPS vertical position anomalies. Geophys. Res. Lett. 41 (17), 6145—6151.

Chinnasamy, P., 2017. Inference of basin flood potential using nonlinear hysteresis effect of basin water storage: case study of the Koshi basin. Hydrol. Res. 48 (6), 1554—1565. Available from: https://doi.org/10.2166/nh.2016.268.

Crow, W.T., Bindlish, R., Jackson, T.J., 2005. The added value of spaceborne passive microwave soil moisture retrievals for forecasting rainfall-runoff partitioning. Geophys. Res. Lett. 32, 18.

Dai, Z., Du, J., Li, J., Li, W., Chen, J., 2008. Runoff characteristics of the Changjiang River during 2006: effect of extreme drought and the impounding of the Three Gorges Dam. Geophys. Res. Lett. 35 (7).

Davidson, E.A., de Araújo, A.C., Artaxo, P., Balch, J.K., Brown, I.F., Bustamante, M.M., et al., 2012. The Amazon basin in transition. Nature 481 (7381), 321.

Diffenbaugh, N.S., Scherer, M., 2011. Observational and model evidence of global emergence of permanent, unprecedented heat in the 20th and 21st centuries. Clim. Change 107, 615—624.

Dijk, A.I., Beck, H.E., Crosbie, R.S., Jeu, R.A., Liu, Y.Y., Podger, G.M., et al., 2013. The Millennium Drought in southeast Australia (2001–2009): natural and human causes and implications for water resources, ecosystems, economy, and society. Water Resour. Res. 49 (2), 1040–1057.
D'Odorico, P., Laio, F., Ridolfi, L., 2010. Does globalization of water reduce societal resilience to drought? Geophys. Res. Lett. 37.
Entekhabi, D., Rodriguez-Iturbe, I., Castelli, F., 1996. Mutual interaction of soil moisture state and atmospheric process. J. Hydrol. 184, 3–17.
Famiglietti, J.S., 2004. Remote sensing of terrestrial water storage, soil moisture and surface waters. State Planet: Front. Challen. geophys. 197–207.
Famiglietti, J.S., 2014. The global groundwater crisis. Nat. Clim. Change 4 (11), 945.
Famiglietti, J.S., Lo, M., Ho, S.L., Bethune, J., Anderson, K.J., Syed, T.H., et al., 2011. Satellites measure recent rates of groundwater depletion in California's Central Valley. Geophys. Res. Lett. 38 (3).
Faunt, C.C., Hanson, R.T., Belitz, K., 2009. Chapter A. Introduction, Overview of Hydrogeology, and Textural Model of California's Central Valley. US Geological Survey professional paper, 1766.
Frappart, F., Papa, F., da Silva, J.S., Ramillien, G., Prigent, C., Seyler, F., et al., 2012. Surface freshwater storage and dynamics in the Amazon basin during the 2005 exceptional drought. Environ. Res. Lett. 7 (4), 044010.
Galloway, D., Riley, F.S., 1999. San Joaquin Valley, California. Land subsidence in the United States: US Geological Survey Circular 1182, 23–34.
García-García, D., Ummenhofer, C.C., Zlotnicki, V., 2011. Australian water mass variations from GRACE data linked to Indo-Pacific climate variability. Remote Sensing Environ. 115 (9), 2175–2183.
García-Herrera, R., Díaz, J., Trigo, R.M., Luterbacher, J., Fischer, E.M., 2010. A review of the European summer heat wave of 2003. Crit. Rev. Environ. Sci. Technol. 40 (4), 267–306.
Getirana, A., 2016. Extreme water deficit in Brazil detected from space. J. Hydrometeorol. 17 (2), 591–599.
Getirana, A., Kumar, S., Girotto, M., Rodell, M., 2017. Rivers and floodplains as key components of global terrestrial water storage variability. Geophys. Res. Lett. 44 (20).
Girotto, M., Margulis, S.A., Durand, M., 2014. Probabilistic SWE reanalysis as a generalization of deterministic SWE reconstruction techniques. Hydrol. Processes 28 (12), 3875–3895.
Girotto, M., De Lannoy, G.J., Reichle, R.H., Rodell, M., 2016. Assimilation of gridded terrestrial water storage observations from GRACE into a land surface model. Water Resour. Res. 52 (5), 4164–4183.
Girotto, M., De Lannoy, G.J., Reichle, R.H., Rodell, M., Draper, C., Bhanja, S.N., et al., 2017. Benefits and pitfalls of GRACE data assimilation: a case study of terrestrial water storage depletion in India. Geophys. Res. Lett. 44 (9), 4107–4115.
Gleeson, T., Wada, Y., Bierkens, M.F., van Beek, L.P., 2012. Water balance of global aquifers revealed by groundwater footprint. Nature 488 (7410), 197.
Groisman, P.Y., Knight, R.W., Karl, T.R., 2012. Changes in intense precipitation over the central United States. J. Hydrometeorol. 13 (1), 47–66.
Hall, D.K., Chang, A.T., Siddalingaiah, H., 1988. Reflectances of glaciers as calculated using Landsat-5 Thematic Mapper data. Remote Sensing Environ. 25 (3), 311–321.
Han, S.C., Shum, C.K., Bevis, M., Ji, C., Kuo, C.Y., 2006. Crustal dilatation observed by GRACE a er the 2004 Sumatra-Andaman earthquake. Science 313, 658–662. Available from: https://doi.org/10.1126/science.1128661.
Hoerling, M., Eischeid, J., Kumar, A., Leung, R., Mariotti, A., Mo, K., et al., 2014. Causes and predictability of the 2012 Great Plains drought. Bull. Am. Meteorol. Soc. 95 (2), 269–282.

Houborg, R., Rodell, M., Li, B., Reichle, R., Zaitchik, B.F., 2012. Drought indicators based on model-assimilated Gravity Recovery and Climate Experiment (GRACE) terrestrial water storage observations. Water Resour. Res. 48 (7).

Humphrey, V., Gudmundsson, L., Seneviratne, S.I., 2016. Assessing global water storage variability from GRACE: trends, seasonal cycle, subseasonal anomalies and extremes. Surveys Geophys. 37 (2), 357–395.

Kirchner, J.W., 2009. Catchments as simple dynamical systems: catchment characterization, rainfall-runoff modeling, and doing hydrology backwards. Wat. Resour. Res. 45, W02429.

Kusche, J., Eicker, A., Forootan, E., Springer, A., Longuevergne, L., 2016. Mapping probabilities of extreme continental water storage changes from space gravimetry. Geophys. Res. Lett. 43 (15), 8026–8034.

Leblanc, M.J., Tregoning, P., Ramillien, G., Tweed, S.O., Fakes, A., 2009. Basin-scale, integrated observations of the early 21st century multiyear drought in southeast Australia. Water Resour. Res. 45 (4).

Li, B., Rodell, M., Zaitchik, B.F., Reichle, R.H., Koster, R.D., van Dam, T.M., 2012. Assimilation of GRACE terrestrial water storage into a land surface model: evaluation and potential value for drought monitoring in western and central Europe. J. Hydrol. 446, 103–115.

Li, B., Rodell, M., Famiglietti, J.S., 2015. Groundwater variability across temporal and spatial scales in the central and northeastern U.S. J. Hydrol. 525, 769–780. Available from: https://doi.org/10.1016/j.jhydrol.2015.04.033.

Li, L., Simonovic, S.P., 2002. System dynamics model for predicting floods from snowmelt in North American prairie watersheds. Hydrol. Process. 16, 2645–2666.

Long, D., Shen, Y., Sun, A., Hong, Y., Longuevergne, L., Yang, Y., et al., 2014. Drought and flood monitoring for a large karst plateau in Southwest China using extended GRACE data. Remote Sensing Environ. 155, 145–160.

Luthcke, S.B., Sabaka, T.J., Loomis, B.D., et al., 2013. Antarctica, Greenland and Gulf of Alaska land ice evolution from an iterated GRACE global mascon solution. J. Glac 59 (216), 613–631. Available from: https://doi.org/10.3189/2013JoG12J147.

Margulis, S.A., Cortés, G., Girotto, M., Huning, L.S., Li, D., Durand, M., 2016. Characterizing the extreme 2015 snowpack deficit in the Sierra Nevada (USA) and the implications for drought recovery. Geophys. Res. Lett. 43 (12), 6341–6349.

Milly, P.C.D., Dunne, K.A., 1994. Sensitivity of the global water cycle to the water-holding capacity of the land. J. Clim. 7, 506–526.

Molodtsova, T., Molodtsov, S., Kirilenko, A., Zhang, X., VanLooy, J., 2016. Evaluating flood potential with GRACE in the United States. Nat. Hazards Earth Syst. Sci. 16 (4), 1011–1018.

Niemeyer, S., 2008. New drought indices. *Options Méditerranéennes*. Série A: Séminaires Méditerranéens 80, 267–274.

Pachauri, R.K., Allen, M.R., Barros, V.R., Broome, J., Cramer, W., Christ, R., et al., 2014. Climate change 2014: synthesis report. Contribution of Working Groups I, II and III to the fifth assessment report of the Intergovernmental Panel on Climate Change (p. 151). IPCC.

Reager, J.T., Famiglietti, J.S., 2009. Global terrestrial water storage capacity and flood potential using GRACE. Geophys. Res. Lett. 36 (23), L23402.

Reager, J.T., Thomas, B.F., Famiglietti, J.S., 2014. River basin flood potential inferred using GRACE gravity observations at several months lead time. Nat. Geosci. 7 (8), 588.

Reager, J.T., Thomas, A.C., Sproles, E.A., Rodell, M., Beaudoing, H.K., Li, B., et al., 2015. Assimilation of GRACE terrestrial water storage observations into a land surface model for the assessment of regional flood potential. Remote Sensing 7 (11), 14663–14679.

Rebetez, M., Mayer, H., Dupont, O., Schindler, D., Gartner, K., Kropp, J.P., et al., 2006. Heat and drought 2003 in Europe: a climate synthesis. Ann. Forest Sci. 63 (6), 569–577.
Richey, A.S., Thomas, B.F., Lo, M.-H., Swenson, S., Rodell, M., Famiglietti, J.S., 2015. Uncertainty in global groundwater storage estimates in a total groundwater stress framework. Wat. Resour. Res. 51, 5198–5216. Available from: https://doi.org/10.1002/2015WR017351.
Rodell, M., 2012. 11 Satellite Gravimetry Applied to Drought Monitoring. Remote Sensing Drought: Innovat. Monit. Approach. 261.
Rodell, M., Famiglietti, J.S., 1999. Detectability of variations in continental water storage from satellite observations of the time dependent gravity field. Water Resour. Res. 35 (9), 2705–2723.
Rodell, M., Famiglietti, J.S., 2001. An analysis of terrestrial water storage variations in Illinois with implications for the Gravity Recovery and Climate Experiment (GRACE). Water Resour. Res. 37 (5), 1327–1339.
Rodell, M., Chao, B.F., Au, A.Y., Kimball, J.S., McDonald, K.C., 2005. Global biomass variation and its geodynamic effects: 1982–98. Earth Interact. 9 (2), 1–19.
Rodell, M., Velicogna, I., Famiglietti, J.S., 2009. Satellite-based estimates of groundwater depletion in India. Nature 460 (7258), 999.
Rowlands, D.D., Luthcke, S.B., Klosko, S.M., Lemoine, F.G., Chinn, D.S., McCarthy, J. J., et al., 2005. Resolving mass flux at high spatial and temporal resolution using GRACE intersatellite measurements. Geophys. Res. Lett. 32 (4).
Sakumura, C., Bettadpur, S., Save, H., McCullough, C., 2016. High-frequency terrestrial water storage signal capture via a regularized sliding window mascon product from GRACE. J. Geophys. Res. Solid Earth 121 (5), 4014–4030.
Save, H., Bettadpur, S., Tapley, B.D., 2012. Reducing errors in the GRACE gravity solutions using regularization. J. Geod. Available from: https://doi.org/10.1007/s00190-012-0548-5.
Sayama, T., McDonnell, J.J., Dhakal, A., Sullivan, K., 2011. How much water can a watershed store? Hydrol. Process. 25, 3899–3908.
Scanlon, B.R., Longuevergne, L., Long, D., 2012a. Ground referencing GRACE satellite estimates of groundwater storage changes in the California Central Valley, USA. Water Resour. Res. 48 (4).
Scanlon, B.R., Faunt, C.C., Longuevergne, L., Reedy, R.C., Alley, W.M., McGuire, V. L., et al., 2012b. Groundwater depletion and sustainability of irrigation in the US High Plains and Central Valley. Proc. Nat. Acad. Sci. 109 (24), 9320–9325.
Scawthorn, C., 1999. Modeling flood events in the US. Proceedings of the EuroConference on Global Change and Catastrophe Risk Management, International Institute for Advanced Systems Analysis, Laxenburg, Austria.
Schmugge, T.J., Kustas, W.P., Ritchie, J.C., Jackson, T.J., Rango, A., 2002. Remote sensing in hydrology. Adv. Water Resour. 25 (8-12), 1367–1385.
Seneviratne, S., 2003. Terrestrial water storage: a critical variable for mid-latitude climate and climate change (Doctoral dissertation, ETH Zurich).
Seneviratne, S.I., Corti, T., Davin, E.L., Hirschi, M., Jaeger, E.B., Lehner, I., et al., 2010. Investigating soil moisture–climate interactions in a changing climate: a review. Earth-Sci. Rev. 99 (3-4), 125–161.
Slater, L.J., Villarini, G., 2016. Recent trends in US flood risk. Geophys. Res. Lett. 43 (24).
Sordo-Ward, A., Bejarano, M.D., Iglesias, A., Asenjo, V., Garrote, L., 2017. Analysis of current and future SPEI droughts in the La Plata Basin based on results from the Regional Eta Climate Model. Water 9 (11), 857.

Sun, A.Y., Scanlon, B.R., AghaKouchak, A., Zhang, Z., 2017a. Using GRACE satellite gravimetry for assessing large-scale hydrologic extremes. Remote Sensing 9 (12), 1287.
Sun, Z., Zhu, X., Pan, Y., Zhang, J., 2017b. Assessing terrestrialwater storage and flood potential using GRACE data in the Yangtze River Basin. China, Remote Sensing 9 (10). Available from: https://doi.org/10.3390/rs9101011.
Sun, Z., Zhu, X., Pan, Y., Zhang, J., Liu, X., 2018. Drought evaluation using the GRACE terrestrial water storage deficit over the Yangtze River Basin, China. Sci. Total Environ. Available from: https://doi.org/10.1016/j.scitotenv.2018.03.292.
Swenson, S., Wahr, J., 2006. Post-processing removal of correlated errors in GRACE data. Geophys. Res. Lett. 33 (8).
Swenson, S., Wahr, J., 2009. Monitoring the water balance of Lake Victoria, East Africa, from space. J. Hydrol. 370 (1-4), 163−176.
Syed, T.H., Famiglietti, J.S., Rodell, M., Chen, J., Wilson, C.R., 2008. Analysis of terrestrial water storage changes from GRACE and GLDAS. Water Resour. Res. 44 (2).
Tangdamrongsub, N., Ditmar, P.G., Steele-Dunne, S.C., Gunter, B.C., Sutanudjaja, E. H., 2016. Assessing total water storage and identifying flood events over Tonlé Sap basin in Cambodia using GRACE and MODIS satellite observations combined with hydrological models. Remote Sensing Environ. 181, 162−173.
Tapley, B.D., Bettadpur, S., Ries, J.C., Thompson, P.F., Watkins, M.M., 2004. GRACE measurements of mass variability in the Earth system. Science 305 (5683), 503−505.
Thomas, A.C., Reager, J.T., Famiglietti, J.S., Rodell, M., 2014. A GRACE-based water storage deficit approach for hydrological drought characterization. Geophys. Res. Lett. 41 (5), 1537−1545.
Wada, Y., van Beek, L.P., van Kempen, C.M., Reckman, J.W., Vasak, S., Bierkens, M. F., 2010. Global depletion of groundwater resources. Geophys. Res. Lett. 37 (20).
Wahr, J., Molenaar, M., Bryan, F., 1998. Time variability of the Earth's gravity field: hydrological and oceanic effects and their possible detection using GRACE. J. Geophys. Res. Solid Earth 103 (B12), 30205−30229.
Wahr, J., Swenson, S., Velicogna, I., 2006. Accuracy of GRACE mass estimates. Geophys. Res. Lett. 33 (6).
Wang, G., Wang, D., Trenberth, K.E., Erfanian, A., Yu, M., Bosilovich, M.G., et al., 2017a. The peak structure and future changes of the relationships between extreme precipitation and temperature. Nat. Clim. Change 7 (4), 268.
Wang, S., Zhou, F., Russell, H.A., 2017b. Estimating snow mass and peak river flows for the mackenzie river basin using grace satellite observations. Remote Sensing 9 (3), 256.
Wang, S.Y., Hakala, K., Gillies, R.R., Capehart, W.J., 2014. The Pacific quasi-decadal oscillation (QDO): an important precursor toward anticipating major flood events in the Missouri River Basin? Geophys. Res. Lett. 41 (3), 991−997.
Watkins, M.M., Wiese, D.N., Yuan, D.N., Boening, C., Landerer, F.W., 2015. Improved methods for observing Earth's time variable mass distribution with GRACE using spherical cap mascons. J. Geophys. Res. Solid Earth 120 (4), 2648−2671.
Yi, H., Wen, L., 2016. Satellite gravity measurement monitoring terrestrial water storage change and drought in the continental United States. Sci. Rep. 6, 19909.
Yirdaw, S.Z., Snelgrove, K.R., Agboma, C.O., 2008. GRACE satellite observations of terrestrial moisture changes for drought characterization in the Canadian Prairie. J. Hydrol. 356 (1-2), 84−92.
Zaitchik, B.F., Rodell, M., Reichle, R.H., 2008. Assimilation of GRACE terrestrial water storage data into a land surface model: results for the Mississippi River basin. J. Hydrometeorol. 9 (3), 535−548.

Zehe, E., Becker, R., Bárdossy, A., Plate, E., 2005. Uncertainty of simulated catchment runoff response in the presence of threshold processes: role of initial soil moisture and precipitation. J. Hydrol. 315 (1-4), 183–202.
Zhao, M., Velicogna, I., Kimball, J.S., 2017. Satellite observations of regional drought severity in the continental United States using GRACE-based terrestrial water storage changes. J. Clim. 30 (16), 6297–6308.
Zhou, H., Luo, Z., Tangdamrongsub, N., Wang, L., He, L., Xu, C., et al., 2017. Characterizing drought and flood events over the Yangtze River Basin using the HUST-Grace2016 solution and ancillary data. Remote Sensing 9 (11). Available from: https://dx.doi.org/10.3390/rs9111100.
dutt Vishwakarma, B., Jain, K., Sneeuw, N., Devaraju, B., 2013. Mumbai 2005, Bihar 2008 flood reflected in mass changes seen by GRACE satellites. J. Indian Soc. Remote Sensing 41 (3), 687–695.

Further reading

Chen, J., Famiglietti, J.S., Scanlon, B.R., Rodell, M., 2016. Groundwater storage changes: present status from GRACE observations. Surveys Geophys. 37 (2), 397–417.
Rippey, B.R., 2015. The US drought of 2012. Weather Clim. Extrem. 10, 57–64.
Svoboda, M., LeComte, D., Hayes, M., Heim, R., Gleason, K., Angel, J., et al., 2002. The drought monitor. Bull. Am. Meteorol. Soc. 83 (8), 1181–1190.
Wang, S., Russell, H.A., 2016. Forecasting snowmelt-induced flooding using GRACE satellite data: a case study for the Red River watershed. Can. J. Remote Sensing 42 (3), 203–213.